

## ORIGINAL ARTICLE

# Characterisation of dehydrated amnion chorion membranes and evaluation of fibroblast and keratinocyte responses in vitro

John P. McQuilling  | MaryRose Kammer  | Kelly A. Kimmerling  | Katie C. Mowry 

Research and Development, Organogenesis Inc., Birmingham, Alabama

## Correspondence

Katie C. Mowry, PhD, 2641 Rocky Ridge Ln, Birmingham, AL 35216.

Email: kmowry@organo.com

## Funding information

Organogenesis, Grant/Award Number: NA

The purpose of this study is to characterise the composition of a dehydrated amnion and chorion graft and investigate how factors released from this graft interact with cells important to the wound microenvironment using in vitro models. Characterisation was completed by proteomic analysis of growth factors and cytokines, evaluation of matrix components and protease inhibition, immunohistochemistry, and in vitro release of key growth factors and cytokines. To evaluate the effect of released factors on cells found within the microenvironment, in vitro assays including: cell proliferation, migration, gene expression, protein production, and intracellular pathway activation were used; additionally, responses of fibroblasts in the context of inflammation were measured. We found that released factors from dehydrated amnion/chorion membranes (dACM) stimulated cell proliferation, migration, and altered gene and protein expression profiles of cells important for wound repair in vitro. When cells were cultured in the presence of pro-inflammatory cytokines, the addition of releasate from dACM resulted in an altered production of cytokines, including a reduction of pro-inflammatory regulated on activation, normal T cell expressed and secreted (RANTES). In sum, the results presented here characterise the components of dACM, and in vitro studies were used to evaluate interactions of dACM with cell types important in wound healing.

## KEYWORDS

amnion, chorion, tissue regeneration, wound repair

## 1 | INTRODUCTION

Chronic wounds represent a significant and growing health care problem, illustrated by the prevalence of diabetic foot

**Abbreviations:** CM, conditioned media; CMFDA, 5-chloromethylfluorescein diacetate; dACM, dehydrated amnion/chorion membranes; DMEM, Dulbecco's modified eagle medium; ECM, extracellular matrix; ELISA, enzyme-linked immunosorbent assay; GAPDH, glyceraldehyde 3-phosphate dehydrogenase; H&E, haematoxylin and eosin; HRP, horseradish peroxidase; ITSE, insulin-transferrin-selenium-ethanolamine; MCP-1, monocyte chemoattractant protein 1; MMP, matrix metalloproteinase; NNGH, N-Isobutyl-N-(4-methoxyphenylsulfonyl)glycyl hydroxamic acid; RANTES, regulated on activation, normal T cell expressed and secreted; sGAGs, sulfated glycosaminoglycans; TBST, tris-based solution in 0.15 M NaCl with 0.1% v/v Triton-X-100.

ulcers (DFUs). Currently, approximately 6 of 100 individuals within the US Medicare population are diagnosed with a DFU, yearly.<sup>1</sup> As diabetes rates are projected to increase worldwide with estimates of up to 592 million individuals by 2035,<sup>1</sup> it is clear that chronic wounds are a significant and growing problem. Failure to heal these wounds often leads to amputation, which significantly increases a patient's risk of death.<sup>1</sup> 1-year mortality rates following lower limb amputation as a result of a diabetic ulcer have been reported to be as high as 40%,<sup>2</sup> highlighting the existing need for advanced therapies to achieve wound closure.

Placental membranes have a long documented history as being used to treat both chronic and acute wounds.<sup>3</sup> Clinical

studies of placental membranes have demonstrated improved outcomes in a variety of wound types, including: acute wounds,<sup>4</sup> DFUs,<sup>5–7</sup> and venous leg ulcers.<sup>8</sup> Placental tissues are processed in various ways, including: cryopreservation, hypothermic storage, and dehydration.<sup>9–11</sup> Composition and processing alters the proteomic composition and may consequently affect how the grafts function.<sup>9,12–15</sup>

There are several beneficial properties that placental membranes natively possess that may support wound healing. In addition to acting as a protective physical covering, placental membranes have been reported to contain a wide variety of growth factors and cytokines,<sup>13</sup> which have been shown to promote beneficial cellular processes *in vitro*.<sup>11,16,17</sup>

The purpose of this study is to characterise the composition of dehydrated amnion/chorion membranes (dACM), detail the release of important factors from dACM, and evaluate how these factors interact with cells important to the wound healing environment using *in vitro* models. To do this, we quantified levels of key growth factors and cytokines present in dACM and measured their release from dACM grafts over 7 days. Additionally, we evaluated specificity of many of these factors within discrete layers within the amnion and chorion tissue. Using *in vitro* models, we evaluated dACM inhibition of protease activity as well as cell responses to dACM.

## 2 | METHODS

### 2.1 | dACM Grafts

dACM (NuShield, Organogenesis Inc., Canton, Massachusetts) is a dehydrated placental-derived graft consisting of all layers of the amnion/chorion membranes. Placentas were donated with informed consent after planned caesarean sections, and all processing was completed in accordance with the Food and Drug Administration's Good Tissue Practices and American Association of Tissue Banks standards. All donors were screened for medical issues, social issues, and communicable diseases that could affect donor suitability. Additionally, prior to release, donors are tested and found to be free of infectious diseases and grafts are terminally sterilised.

### 2.2 | Quantification of key growth factors, cytokines, and ECM components in dACM

Proteomic analysis of dACM was conducted as described in detail elsewhere.<sup>11</sup> Briefly, a custom quantitative multiplex enzyme-linked immunosorbent assay (ELISA) proteomics microarray (Raybiotech Inc, Norcross, Georgia) was used to quantify growth factors and cytokines within dACM. For these arrays, targets were selected, which have been previously shown to be present within placental tissues and are known to be relevant to wound repair processes.<sup>13,18</sup>

### Key Messages

- dehydrated amnion/chorion grafts contain a wide variety of growth factors and cytokines relevant to tissue repair
- the purpose of this study is to characterise the composition of a dehydrated amnion/chorion graft and investigate how factors released from these grafts interact with the cells important to the wound microenvironment using *in vitro* models
- *in vitro*, we found that released factors from dehydrated amnion/chorion membranes (dACM) stimulated cell proliferation, migration, and altered gene and protein expression profiles of cells were important for wound repair. When cells were cultured in the presence of pro-inflammatory cytokines, the addition of dACM resulted in an altered response, including reduction of pro-inflammatory RANTES

dACM grafts from 15 human donors were first minced with a scalpel and then homogenised using a Retsch cryomill (Verder Scientific, Inc., Newtown, Pennsylvania) and incubated overnight in total protein extraction buffer with a protease inhibitor cocktail (EMD Millipore, Burlington, Massachusetts) at 4°C with agitation. Following overnight incubation, the supernatant was removed and loaded into microarray chambers and the assay was run per the manufacturer's instructions.

Additionally, key extracellular matrix (ECM) proteins were quantified within dACM samples using colorimetric kits including collagen (Sircol Soluble Collagen Assay), sulfated glycosaminoglycans (sGAGs, Blyscan Glycosaminoglycan Assay), hyaluronic acid (Purple-Jelly Hyaluronan Assay), and elastin (Fastin Elastin Assay) from Biocolor (Carrickfergus, United Kingdom) per the manufacturer's instructions.

### 2.3 | Quantification of protease inhibition

Inhibition of matrix metalloproteinases (MMP) 2 and MMP-9 protease activity was evaluated using the MMP-2 and MMP-9 fluorometric drug discovery kits (Enzo Life Sciences, Inc., Farmingdale, New York). For these experiments, 5 donors of dACM were evaluated in quadruplicate. dACM was homogenised using a Retsch cryomill, and then incubated at a concentration of 1 cm<sup>2</sup> dACM per 350 μL MMP-2 (3.28 U/μL) or MMP-9 (2.68 U/μL) solution for 30 minutes at 37°C along with the positive control (MMP enzymes alone) and inhibitor control, which consisted of MMP enzymes with a known inhibitor of proteases N-Isobutyl-N-(4-methoxyphenylsulfonyl)glycyl hydroxamic acid (NNGH). Samples were then incubated with a fluorogenic substrate per the manufacturer's instructions in a microplate reader over a 10-minute period and fluorescence was measured (excitation/emission = 328/420) at 1-minute intervals.

Resulting values were then converted to picomoles of substrate hydrolyzed per minute.

## 2.4 | Histology and immunohistochemistry

To evaluate the overall structure and determine the distribution of growth factors and cytokines within sub-layers of dACM, grafts were fixed in 4% neutral-buffered formalin and then paraffin embedded. Serial sections 5  $\mu\text{m}$  thick were cut from the tissue blocks and placed onto charged glass slides (Super-Frost Plus, Fisher Scientific, Pittsburgh, Pennsylvania) and dried overnight at 60°C. Sections were then stained with histologic stains using standard techniques including: haematoxylin and eosin (H&E), Alcian Blue, and Verhoeff-Van Gieson.

For immunohistochemistry, collagen I, collagen III, fibronectin, laminin, hyaluronic acid, TIMP-1, VEGF, bFGF, TGF- $\beta$ 1, IL-1Ra, HGF, and IGF-1 were evaluated. Samples were first deparaffinised and hydrated via graded concentrations of ethanol to deionised water. Details of antigen retrieval methods, primary and secondary antibodies used, and corresponding dilutions can be found in Supporting Information Table S1. After antigen retrieval, sections were washed with deionised water and transferred to a 0.05 M Tris-based solution in 0.15 M NaCl with 0.1% v/v Triton-X-100, pH 7.6 (TBST), blocked using endogenous peroxidase with 3% hydrogen peroxide for 20 minutes, and non-specific background staining was further reduced by incubating slides in 3% normal goat serum for 30 minutes (Sigma-Aldrich, St. Louis, Missouri) at room temperature. Then, slides were incubated at 4°C overnight with appropriate antibodies. Negative controls were produced by eliminating the primary antibodies from the diluents. Slides were washed with TBST, and then incubated with the corresponding secondary antibodies conjugated with horseradish peroxidase. For the chromogen, diaminobenzidine (Scy Tek Laboratories, Logan, Utah) was used and sections were counterstained with haematoxylin (Richard-Allen Scientific, Kalamazoo, Michigan). Samples were imaged with 20 $\times$  and 40 $\times$  objectives on an inverted microscope (Nikon Eclipse Ti, Tokyo, Japan; Nikon, Melville, New York).

## 2.5 | Growth factor and cytokine release

To measure the release of growth factors and cytokines from dACM, grafts from four human donors were cultured in serum-free media consisting of Dulbecco's Modified Eagle Medium (DMEM), supplemented with 1 mg/mL human albumin, L-glutamine, and insulin-transferrin-selenium-ethanolamine (ITSE) at a concentration of 1 mL media per 1  $\text{cm}^2$  at 37°C with gentle rocking. At 0.5, 1, and 3 days, the media were collected, stored at -80°C, and replaced with fresh serum-free media. At 7 days, both the media and graft were collected and stored at -80°C. Grafts were homogenised via cryomill and protein extracted using a Total

Protein Extraction Kit as described above. Released growth factor and cytokine content in the spent media and remaining in grafts were evaluated using a custom quantitative multiplex ELISA proteomics microarray described above. Cumulative release was then calculated and reported as a percent of the total growth factor and cytokines measured.

## 2.6 | Cell culture and media

For all in vitro cell assays, experiments were conducted with a minimum of three distinct cell lines per cell type. Adult human dermal fibroblasts were purchased from Lonza, (Lonza, Walkersville, Maryland) and were maintained in FGM-2 Growth Media prior to sub culturing; passages 3 to 10 were used for all experiments. Adult human epidermal keratinocytes were purchased from Lonza and Life Technologies (Carlsbad, California) and were maintained in Epilife with human keratinocyte growth supplement. Passages 3 to 8 were used for experiments.

Assay media was a reduced-serum media but exact composition varied depending on the cell type and experiment. For both proliferation and gene expression experiments, assay media used for fibroblasts consisted of 10% growth media (FGM-2 Growth Media) in basal media (FBM-2) and for keratinocytes the assay media consisted of DMEM:F12 (Hyclone, Pittsburgh, Pennsylvania) supplemented with 5% fetal bovine serum (FBS) (Corning, Corning, New York) and 1% antibiotic-antimycotic solution (Corning, 30-004). For migration experiments, for both cell types, the assay media consisted of DMEM:F12 supplemented with 0.25% FBS and 1% antibiotic-antimycotic solution. Assay media used for phosphorylation experiments consisted of DMEM:F12 supplemented with ITSE (InVitria, Fort Collins, Colorado), 1% antibiotic-antimycotic solution, and 0.25% FBS. For each experiment, 100% conditioned media (CM) were generated by incubating dACM in appropriate assay media (detailed above) at a concentration of 1  $\text{cm}^2$  dACM per mL media for 3 to 5 days at 4°C with gentle rocking. Ranges of 50% to 10% dACM CM were subsequently made by dilution in appropriate assay media and used for experiments.

## 2.7 | Cell proliferation

Cell proliferation experiments were conducted as previously described in detail.<sup>11</sup> Briefly, fibroblasts and keratinocytes were cultured with 50%, 25%, and 10% (vol/vol) dACM CM for 14 days (fibroblasts) or 10 days (keratinocytes) under standard conditions. For fibroblasts and keratinocytes, cell proliferation ( $n = 6$  per cell line) was assessed using AlamarBlue (ThermoFisher Scientific, Pittsburgh, Pennsylvania). Reduction of the AlamarBlue reagent was compared with controls with known cell numbers in order to determine the number of cells per well at each time point.

## 2.8 | Cell migration

Migration of fibroblasts and keratinocytes was evaluated using a standard Boyden chamber assay ( $n = 3$  per cell line). Transwell inserts were coated with  $5 \mu\text{g/mL}$  of fibronectin (Fisher Scientific) overnight at  $4^\circ\text{C}$  and then rinsed three times with phosphate buffered saline (PBS). For fibroblasts,  $0.5 \text{ cm}^2$  or  $0.25 \text{ cm}^2$  dACM intact pieces and assay media were added to the bottom of reservoirs to incubate overnight at  $37^\circ\text{C}$ . For keratinocytes, 50% or 25% dACM CM were added to the bottom of reservoirs immediately prior to the start of the assay. Fibroblasts were serum-starved overnight. Upon the start of the assay, all cells were trypsinized and added to the top of the inserts ( $150\,000$  cells/well). Plates were incubated under standard culture conditions for 24 hours.

Non-migrating cells were removed using a cotton tip applicator, and cells that had migrated were fixed with 4% paraformaldehyde for 10 minutes prior to staining with a  $50 \mu\text{g/mL}$  crystal violet solution in 20% methanol for 30 minutes at room temperature. Inserts were then rinsed thrice in distilled water and imaged using an inverted microscope (Nikon). For experiments using keratinocytes, images were used to quantify the number of cells that had migrated through the insert using Image J software (NIH, Bethesda, Maryland). For migration experiments with fibroblasts, crystal violet stain was extracted using 30% acetic acid solution and  $100 \mu\text{L}$  of the extracted dye was then pipetted into a 96-well plate in duplicate and the absorbance was measured at  $590 \text{ nm}$  using a standard plate reader. The total number of migrated cells was then determined by comparing the absorbance to a standard curve with a known cell number. For both, migrated cells were normalised to the number of cells that migrated in the assay media group.

## 2.9 | Gene expression

Gene expression was evaluated ( $n = 3$  per cell line) by culturing fibroblasts and keratinocytes in 6-well plates in assay media with and without 25% dACM CM. At 24 hours, 48 hours, and 72 hours, cell supernatant was collected and cell monolayers were collected in RNeasy; all samples were stored at  $-80^\circ\text{C}$  until use. Total RNA was extracted using the Direct-zol RNA micro prep kit (Zymo Research, Irvine, California) and quantified on a NanoDrop 2000 UV/Vis spectrophotometer (Thermo Scientific, Waltham, Massachusetts). Reverse transcription to cDNA was performed using the Verso cDNA synthesis kit (ThermoFisher Scientific). Levels of mRNA were measured using TaqMan probes on a Quantstudio 3 PCR System (Applied Biosystems, Waltham, Massachusetts). Each experimental gene was normalised to glyceraldehyde 3-phosphate dehydrogenase and the relative expression of mRNAs was calculated using the  $2^{-\Delta\Delta\text{Ct}}$  method. A complete list of targets and their accession numbers is given in Table S2.

## 2.10 | ELISAs

Based on the identified changes in gene expression, protein was measured for select upregulated targets using ELISAs. For fibroblasts, ELISAs for IGF-1, IL-6, and KGF were conducted on all frozen supernatant samples ( $n = 3$  per cell line). For keratinocytes, ELISAs were conducted for TGF $\beta$ -1, HB-EGF, IL-1ra, and VEGF ( $n = 3$  per cell line). All ELISAs used were Quantikine ELISA kits (R&D Systems, Minneapolis, Minnesota) and were run according to manufacturer's instructions. For each ELISA, CM alone was evaluated and subtracted from the final results.

## 2.11 | Pathway analysis

Activation of intracellular pathways was measured using ELISA kits to measure total and phosphorylated c-Jun, ERK1/2, SMAD2, and AKT. For these experiments, at least  $n = 3$  per cell line was evaluated (15 minute time point  $n = 3$ , 1 replicate per cell line). Cells were seeded into 6-well plates at  $100\,000$  cells/well and allowed 4 to 8 hours to attach in growth media. Cells were then serum starved overnight in assay media. Cell monolayers were then rinsed with PBS and media replaced with assay media consisting of DMEM:F12 supplemented with Insulin-Transferrin-Selenium (ITS) and 0.25% FBS with or without 50% dACM CM. Cells were then cultured under standard conditions for 15 minutes, 60 minutes, 180 minutes, or 360 minutes. At each time point, cell monolayers were collected in RIPA buffer (ThermoScientific, Waltham, Massachusetts) with Halt Protease and Phosphatase Inhibitor Cocktail (ThermoScientific). Samples were centrifuged at  $14\,000g$  for 15 minutes and supernatants were collected and stored at  $-80^\circ\text{C}$ . Total protein content was quantified for each sample using a Pierce BCA assay (ThermoFisher, Waltham, Massachusetts). Lysates were evaluated at protein concentrations of  $500 \mu\text{g/mL}$  for AKT, C-Jun, and SMAD2 and  $100 \mu\text{g/mL}$  for ERK 1/2. The ratio of phosphorylated protein to total protein absorbance was then calculated and used to evaluate differences between groups.

## 2.12 | Effects of dACM on cellular response to inflammation

Fibroblasts were cultured in the presence of inflammatory cytokines (TNF- $\alpha$  or IL-1 $\beta$ ) with or without CM ( $n = 3$  per cell line). A total of  $40\,000$  fibroblasts were seeded per well into 6-well plates with growth media and cultured overnight under standard culture conditions. Following overnight incubation, growth media were removed and monolayers rinsed with PBS. Fibroblasts were then cultured in assay media alone or in assay media containing TNF- $\alpha$  or IL-1 $\beta$  (1 or  $0.1 \text{ ng/mL}$ ) with or without dACM CM (50% vol/vol). The concentrations of inflammatory cytokines used in this study were determined based on existing literature.<sup>19</sup> At the end of

96 hours, the supernatant was collected and stored at  $-80^{\circ}\text{C}$ . Cell number per well was quantified using AlamarBlue prior to collection with RNazol for qRT-PCR. AlamarBlue assays and PCR were conducted as described above. The frozen supernatant was evaluated using ELISAs for production of regulated on activation, normal T cell expressed and secreted (RANTES) and MCP-1 per the manufacturer's instructions (Invitrogen, Carlsbad).

### 2.13 | Data analysis and statistics

For proliferation, migration, qPCR, and ELISAs, statistical analysis was conducted using a one-way ANOVA with a post-hoc Bonferroni's test where  $P < 0.05$  was considered significant. Comparisons of interest were experimental groups compared with the assay media (or negative control group), independently at each time point. For pathway analysis experiments, paired  $t$  tests were used to compare controls with CM for each cell type and for experiments evaluating the effects of dACM on the cellular response to inflammation, unpaired  $t$  tests were used to compare the effects of CM for each culture condition. For all figures, unless otherwise noted data are reported as average  $\pm$  SD, \* denotes  $P < 0.05$ , \*\* denotes  $P < 0.01$ , and  $\diamond$  denotes  $P < 0.001$ .

## 3 | RESULTS

Proteomic analysis of dACM grafts confirmed physiologically relevant concentrations of all growth factors and cytokines measured (Figure 1A-C). Of the 25 growth factors and cytokines evaluated, insulin-like growth factor-binding protein 1 (IGFBP-1), insulin-like growth factor-1 (IGF-1), and galectin-7 (GAL-7) were present in the highest concentrations ( $20\text{ ng/cm}^2$ ,  $8.2\text{ ng/cm}^2$ , and  $3\text{ ng/cm}^2$ , respectively). Additionally, ECM proteins in dACM were quantified (Figure 1D); these analyses showed high levels ( $\mu\text{grams/cm}^2$ ) of collagen, sGAGs, hyaluronic acid, and elastin. ECM components collagen and elastin were found at the highest concentrations ( $386.65$  and  $137.07\text{ }\mu\text{g/cm}^2$ , respectively). To evaluate the activity of protease inhibitors within the grafts, protease inhibition was quantitatively measured (Figure 1E-F). dACM resulted in significantly reduced MMP-2 and MMP-9 activity compared with the control.

Qualitatively, we evaluated the distribution of ECM proteins as well as key growth factors and cytokines throughout dACM grafts (Figure 2). ECM proteins including: collagen I, collagen III, fibronectin, laminin, hyaluronic acid, and glycosaminoglycans (Alcian Blue stain) were found throughout the dACM graft. Collagen I, collagen III, and fibronectin were highly concentrated in the chorion layer; while laminin was found more predominantly in the amnion layer. Hyaluronic acid was found in high concentrations in the spongy

layer, which makes up the bottom layer of the amnion that interfaces with the chorion, and in the chorion layers of the graft. TIMP-1 was identified predominantly in the chorion. VEGF and bFGF were identified in the endothelial layer of the amnion and in the chorion. IL-1ra and IGF-1 were located primarily in the amnion and were concentrated in the spongy layer of the amnion, and TGF- $\beta$ 1 and HGF were found throughout dACM but were present in high concentrations within the spongy layer. Higher magnification images of VEGF, IL-1ra, and HGF (Figure 2B) illustrate examples of proteins concentrated in the chorion, spongy layer, or amnion.

When measuring the growth factor release from dACM grafts in vitro, the majority of the growth factors measured in this study were released by 7 days. At the 12-hour time point, there was a burst release of  $32.3\% \pm 8.2\%$  of all growth factors and cytokines measured, and by 7 days, an average of  $94.2\% \pm 0.9\%$  of growth factors and cytokines were released from dACM in vitro (Figure 3A). Release curves for select individual targets were graphed (Figure 3B-D). The majority of factors show greater than 90% release by 7 days, but some targets did not release more than 50% in the 7 day period, including: IGFBP-5, TNF $\alpha$ , and PDGF-BB, which released  $45.9\% \pm 53.0\%$ ,  $27.3\% \pm 47.3\%$ , and  $40.9 \pm 10.8\%$ , respectively.

The in vitro responses of human dermal fibroblasts were measured by treating fibroblasts with CM from dACM (Figure 4). Proliferation of fibroblasts was significantly increased compared with the control group (when treated with CM), with significant effects seen as early as the 3-day time point for CM concentrations of 50% and 25%. By 14 days, cell proliferation for all three CM groups was significantly increased over the assay media control group by  $189\% \pm 171\%$ ,  $319\% \pm 285\%$ , and  $201\% \pm 191\%$  for 50%, 25%, and 10% CM groups, respectively (Figure 4A,B,  $n = 18$ ). Boyden chamber assays were used to evaluate fibroblast migration in response to dACM CM; after 24 hours,  $0.5\text{ cm}^2$  and  $0.25\text{ cm}^2$  of dACM resulted in a significant increase in cell migration above assay media controls,  $237\% \pm 112\%$  and  $164\% \pm 103\%$ , respectively (Figure 4C,D,  $n = 9$ ).

Eleven targets were evaluated for gene expression and are presented in Figure 4E; of these targets, bFGF, IGF-I, IL-6, KGF, and VEGF were found to be upregulated in response to dACM CM. COL1, fibronectin (FN), TGF- $\beta$ 1, and TGF- $\beta$ 3 were downregulated in response to dACM. Expression of other targets, including COL3 and HGF, was transiently regulated in this model. Of these targets, protein production levels were measured for targets with the highest levels of upregulation of gene expression (IGF-1, IL-6, and KGF). Significantly increased protein production was seen for both IL-6 (Figure 4F) and KGF (Figure 4G) in response to CM from dACM compared with assay media at all time

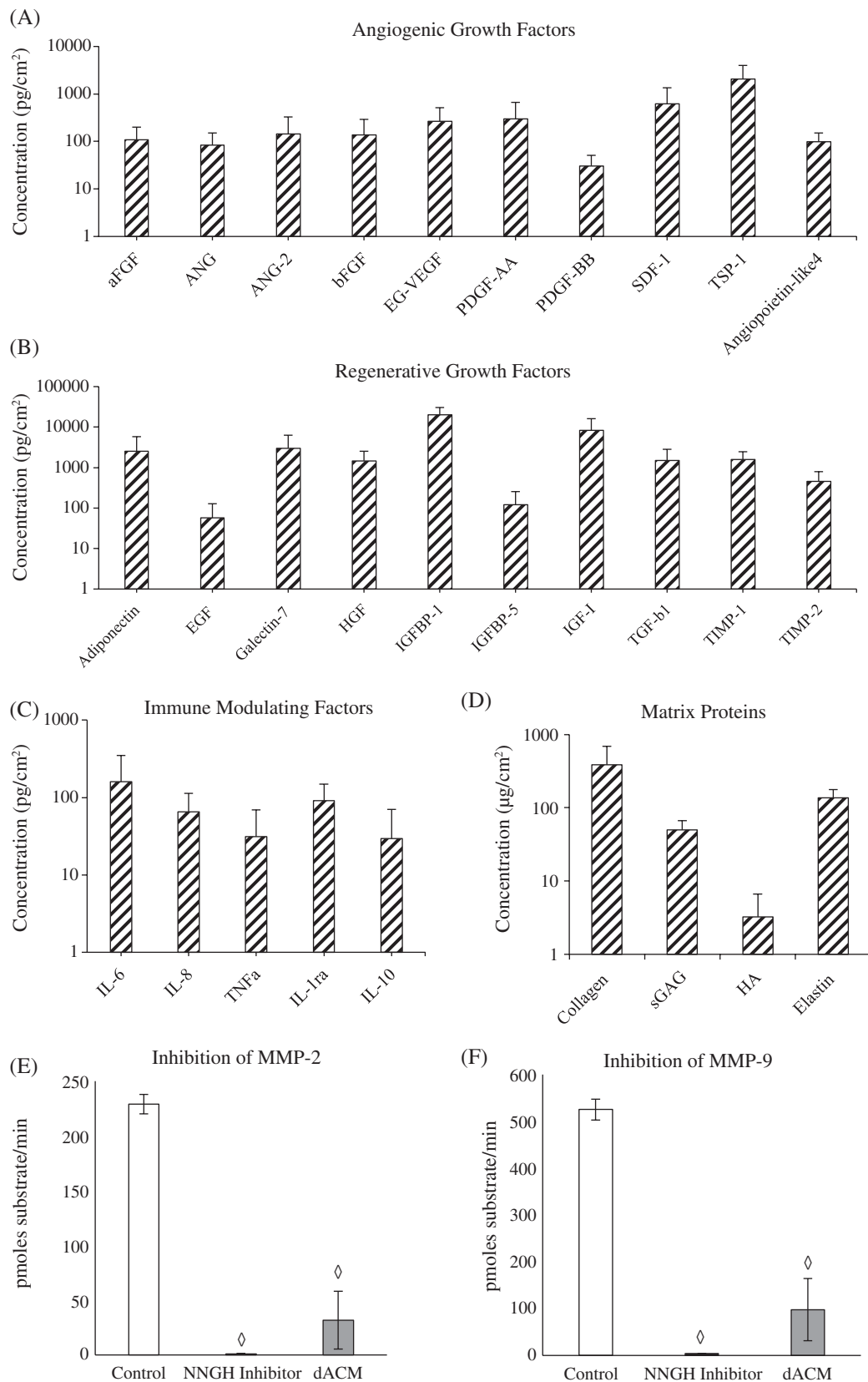


**FIGURE 1** Multiplex enzyme-linked immunosorbent proteomic microarray evaluation of dACM grafts and evaluation of dACM protease inhibition of MMP-2 and MMP-9 in vitro. dACM grafts from 15 human donors were assessed for 25 targets relevant to native wound healing. Results shown here are categorised into groups (A) angiogenic growth factors, (B) regenerative growth factors, (C) immune-modulating factors, and (D) matrix proteins. Reduction of MMP-2 activity (E), and reduction of MMP-9 activity (F) with the addition of dACM. Average  $\pm$  SD,  $\diamond$  denotes  $P < 0.001$ . Abbreviations: dACM, dehydrated amnion/chorion membranes; MMP, matrix metalloproteinase; NNGH, N-Isobutyl-N-(4-methoxyphenylsulfonyl)glycyl hydroxamic acid

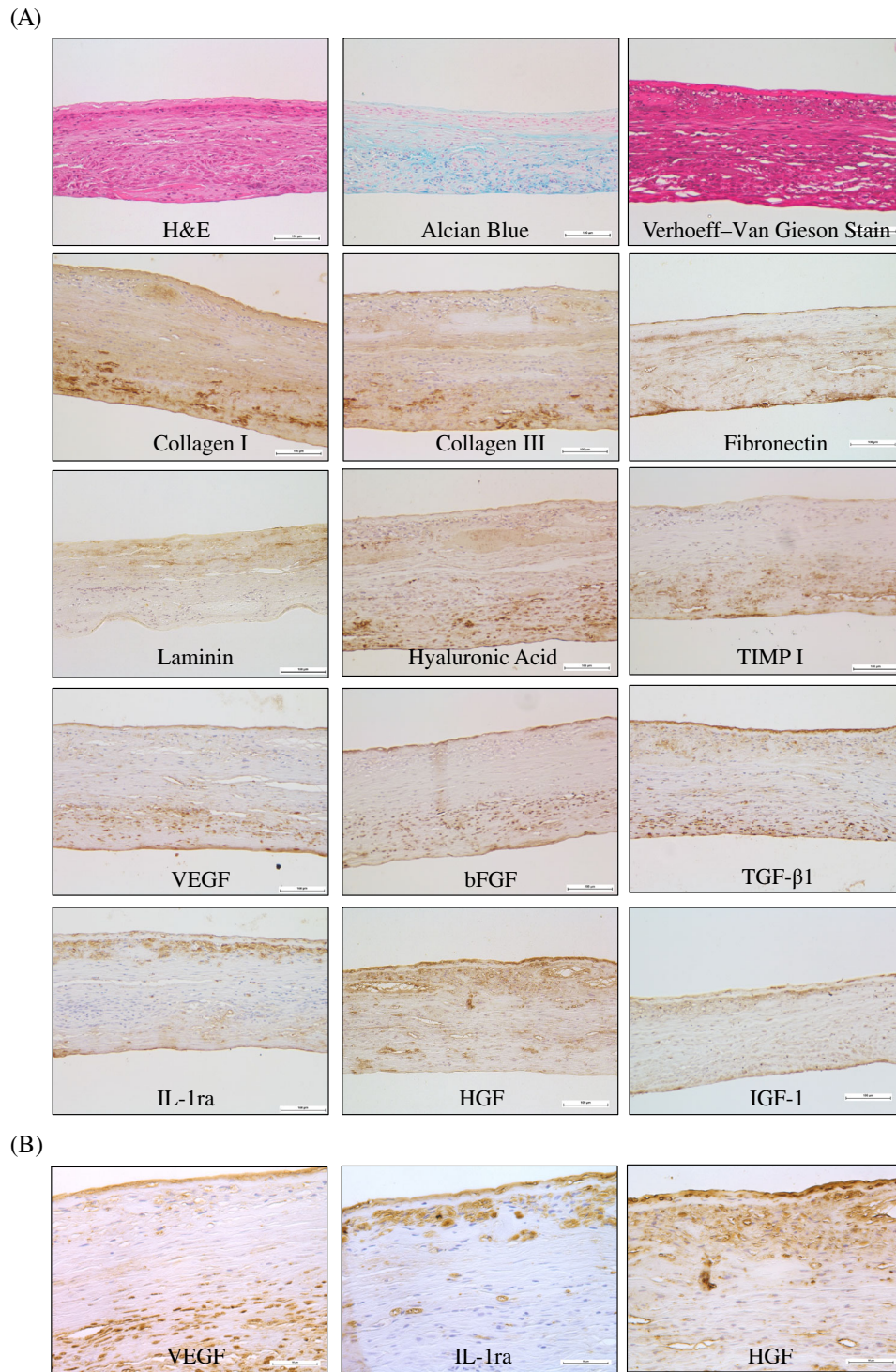


**FIGURE 2** Histological evaluation of dACM grafts. dACM grafts were evaluated using standard histological techniques including: Haematoxylin and Eosin, Alcian Blue, and Verhoeff-Van Gieson. Additionally, representative images of immunohistochemical staining of key extracellular matrix proteins, growth factors, and cytokines in dACM grafts are shown. A, Images taken with a 20 $\times$  objective, each scale bar measures 100  $\mu$ m. B, Select images taken with a 40 $\times$  objective, each scale bar measures 50  $\mu$ m. Abbreviations: dACM, dehydrated amnion/chorion membranes

points. IGF-1 did not show significant changes in protein production (data not shown).

Activation of fibroblast signalling pathways including c-Jun, ERK1/2, SMAD2, and AKT were evaluated after exposure to dACM CM in vitro (Figure 4H). When exposed to CM from dACM, C-Jun phosphorylation was significantly increased compared with controls at 15 minutes

(57%  $\pm$  36%). ERK1/2 phosphorylation was significantly increased compared with controls at the 60-minute time point (64%  $\pm$  70%). SMAD2 phosphorylation was significantly increased compared with controls at both the 15 and 180-minute time points (30%  $\pm$  16% and 17%  $\pm$  21%). AKT phosphorylation was significantly increased at the 15-minute time point (44%  $\pm$  44%). For all pathways,

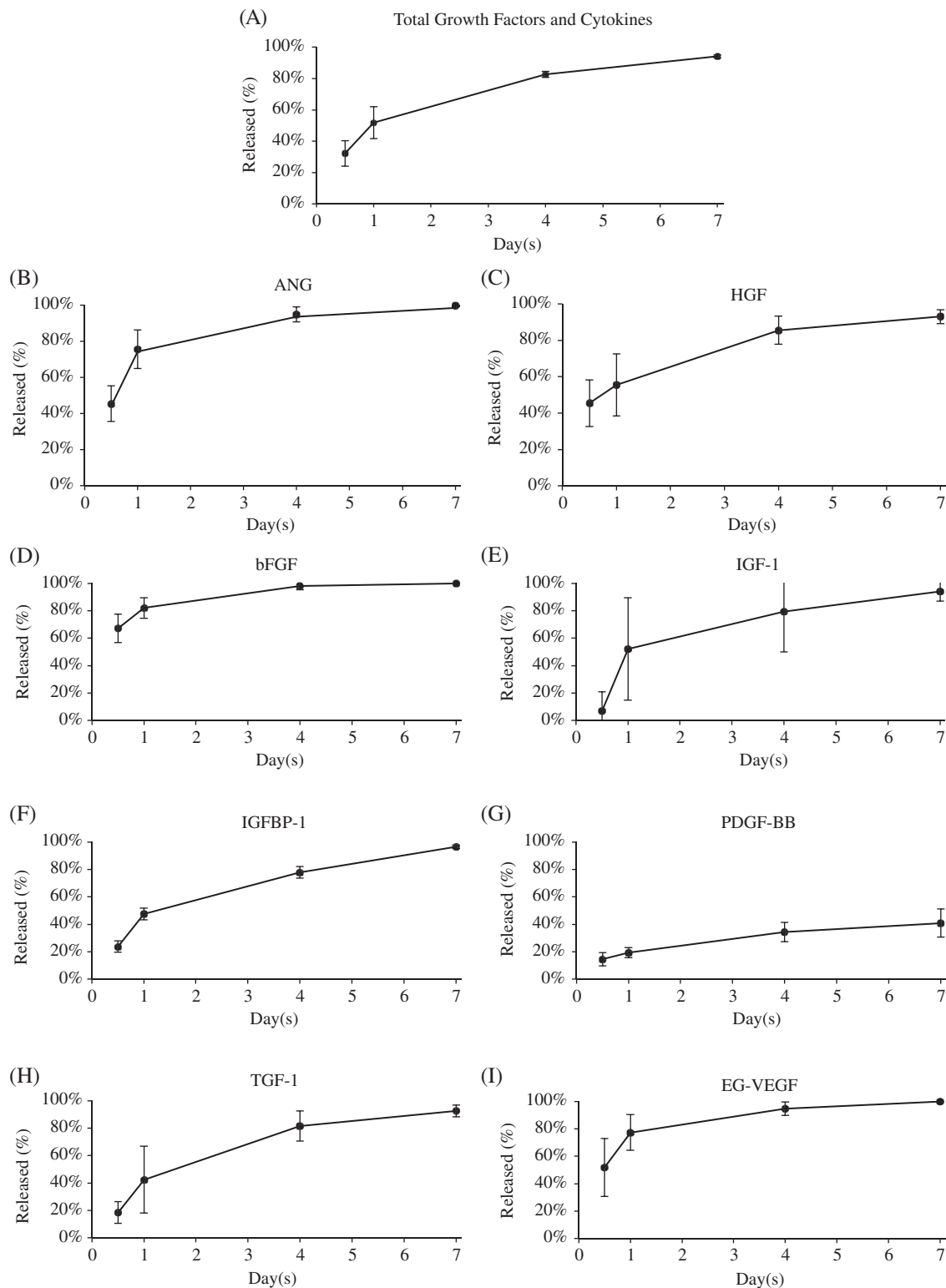


**FIGURE 3** Evaluation of release of growth factor and cytokines from dACM graft. Results here are cumulative release and are presented as average  $\pm$  SD from four human dACM donors. Results are presented as (A) total growth factors and cytokines, (B) angiopoietin (ANG), (C) hepatocyte growth factor (HGF), (D) basic fibroblast growth factor (bFGF), (E) insulin-like growth factor I (IGF-I), (F) insulin-like growth factor-binding protein 1 (IGFBP-1), (G) platelet-derived growth factor BB (PDGF-BB), (H) transforming growth factor beta 1 (TGF- $\beta$ 1), and (I) endocrine gland-derived vascular endothelial growth factor (EG-VEGF). Abbreviations: dACM, dehydrated amnion/chorion membranes

phosphorylation levels returned to baseline levels by 360 minutes.

Adult human epidermal keratinocyte responses to dACM CM were evaluated in vitro (Figure 5). Keratinocyte

proliferation increased in response to CM from dACM as early as 3 days with 50, 25, and 10% CM (Figure 5A). These increases were seen out to 10 days qualitatively (Figure 5B) and quantitatively with 50% and 25% dACM CM groups



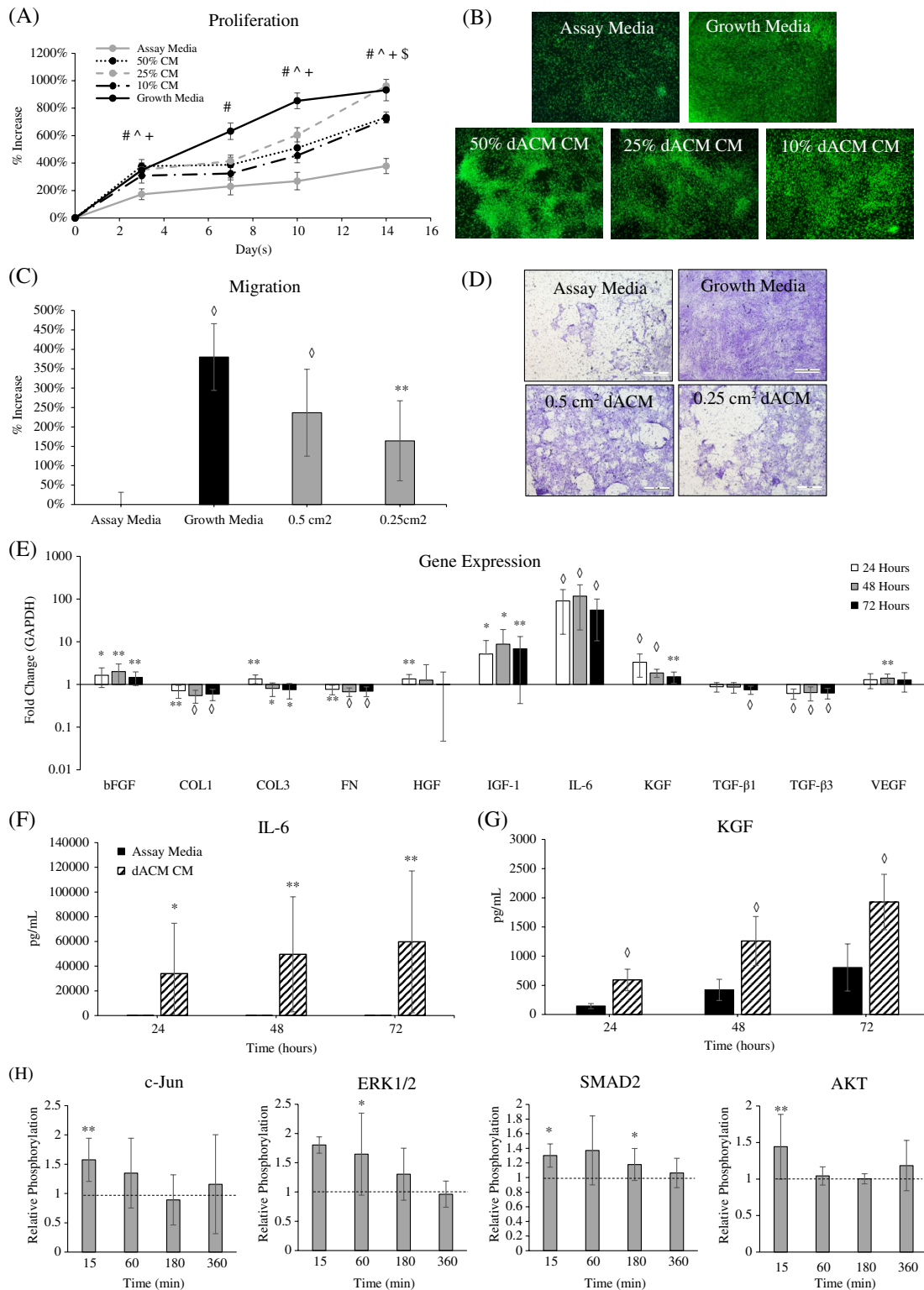


**FIGURE 4** Evaluation of dACM on adult human dermal fibroblasts in vitro. A, proliferation of fibroblasts (average  $\pm$  SEM); significance compared with assay media was denoted as: # for growth media; ^ for 50% dACM CM, + for 25% dACM CM, and \$ for 10% dACM CM (B) representative images of fibroblasts at 14-days stained with 5-chloromethylfluorescein diacetate (CMFDA) and DAPI; C, migration of fibroblasts in response to dACM (0.5 cm<sup>2</sup> or 0.25 cm<sup>2</sup>); D, representative images of migrated cells shown stained with crystal violet; E, gene expression changes at 24, 48, and 72 hours; protein production levels of IL-6 (F) and KGF (G) over 72 hours; and H, relative phosphorylation/total protein in response to dACM (relative to assay media). Average  $\pm$  SD, significance compared with assay media is denoted by: \* denotes  $P < 0.05$ , \*\* denotes  $P < 0.01$ , and  $\diamond$  denotes  $P < 0.001$ . Abbreviations: CM, conditioned media; dACM, dehydrated amnion/chorion membranes; GAPDH, glyceraldehyde 3-phosphate dehydrogenase

maintaining a significant increase in cell proliferation compared with assay media control groups with 240%  $\pm$  66% and 242%  $\pm$  58%, respectively (Figure 5A). Migration of

keratinocytes in response to dACM CM showed trends for increases but these changes were not statistically significant (Figure 5C,D).

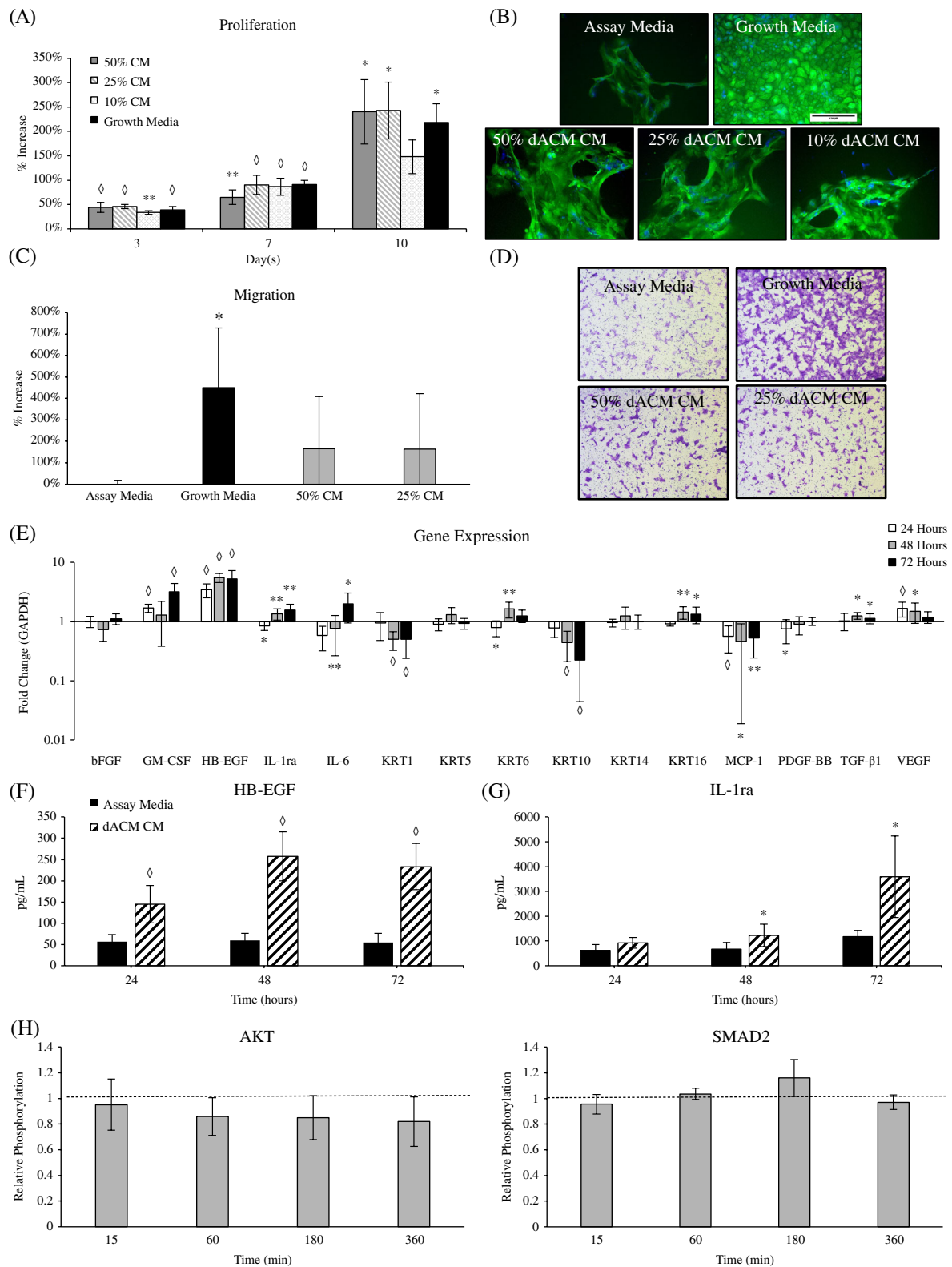


**FIGURE 5** Evaluation of dACM on adult human epidermal keratinocytes in vitro. A, proliferation of keratinocytes (Average  $\pm$  SEM); B, representative images of keratinocytes stained with CMFDA and DAPI for 10 days; C, migration of keratinocytes in response to dACM CM; D, representative images of migrated cells shown stained with crystal violet; E, gene expression changes at 24, 48, and 72 hours; protein production levels of HB-EGF (F) and IL-1ra (G) over 72 hours; and H, relative phosphorylation/total protein in response to dACM (relative to assay media). Average  $\pm$  SD, significance compared with assay media is denoted by: \* denotes  $P < 0.05$ , \*\* denotes  $P < 0.01$ , and  $\diamond$  denotes  $P < 0.001$ . Abbreviations: CM, conditioned media; dACM, dehydrated amnion/chorion membranes

Fifteen genes and their expression over 72 hours were evaluated with and without dACM CM, the results are presented as fold change to assay media controls (Figure 5E). GM-CSF, HB-EGF, and VEGF were upregulated compared with assay media controls; IL-1Ra, IL-6, and TGF- $\beta$ 1 were initially either downregulated or unaltered but were significantly upregulated by 72 hours. We found significant upregulation of genes related to keratinocyte activation, including: KRT6 (at 48 hours) and KRT16 (at 48 and 96 hours). MCP-1 was consistently downregulated; KRT-1 was downregulated at 48 and 72 hours; and PDGF-BB was significantly downregulated at 24 hours only. Of these, protein production levels were measured for targets with the highest levels of upregulation of gene expression (TGF- $\beta$ 1, HB-EGF, IL-1ra, and VEGF). Keratinocyte production of HB-EGF and IL-1ra closely matched gene expression changes, where production of HB-EGF was significantly increased in dACM CM groups compared with controls at all three time points ( $n = 8$ , Figure 5F). IL-1Ra production was unchanged at the 24-hour time point, but significantly increased in dACM CM at the 48-hour and 72-hour time points compared with controls ( $n = 6$ , Figure 5G). TGF- $\beta$ 1 and VEGF did not show significant changes in protein production (data not shown).

Of the pathways evaluated in this study, only SMAD2 and AKT phosphorylation was noticeably altered following exposure to dACM CM in vitro (Figure 5H). The addition of dACM CM resulted in a decrease in AKT phosphorylation compared with controls at all time points (Figure 5H). Cells exposed to dACM CM had a slight, but not significant, increase in SMAD2 phosphorylation (compared with controls) at 60 minutes and 180 minutes.

The addition of TNF- $\alpha$  or IL-1 $\beta$  cytokines to fibroblasts resulted in an upregulation in the expression and production of pro-inflammatory molecule, RANTES (Figure 6A-D). Of note, dACM CM in the assay media group (no inflammation) resulted in a small but significant increase in gene expression and production of RANTES in all groups. The addition of dACM CM to inflammatory groups resulted in trends for decreased expression of RANTES across all groups and a significant decrease in RANTES expression in the 1 ng/mL TNF- $\alpha$  ( $n = 9$ , Figure 6A) and 0.1 ng/mL IL-1 $\beta$  groups ( $n = 9$ , Figure 6C). The addition of dACM CM to 1 ng/mL TNF- $\alpha$  and 0.1 ng/mL IL-1 $\beta$  groups led to a significant reduction in RANTES production ( $n = 12$ , Figure 6B&D).

The addition of TNF- $\alpha$  or IL-1 $\beta$  at 1 ng/mL resulted in increased expression and production of monocyte chemoattractant protein 1, MCP-1. Lower concentrations of inflammatory stimulus alone led to a small increase or no change to MCP-1 expression and production. Interestingly, MCP-1 gene expression and production were increased in assay media groups stimulated with dACM and no inflammation (Figure 6E-H). MCP-1 production and expression from fibroblasts were significantly increased when dACM CM

was added in TNF- $\alpha$  groups ( $n = 9$ , Figure 6E,F). Conversely, when stimulated with IL-1 $\beta$  and dACM, there were no significant changes in gene expression (Figure 6G); despite this, the addition of dACM CM was found to significantly decrease the production of MCP-1 in the 1 ng/mL IL-1 $\beta$  group ( $n = 9$ , Figure 6H).

## 4 | DISCUSSION

In this study, we found that dACM contains a variety of ECM proteins, growth factors, and cytokines. We found specificity of several factors to the epithelial layer, chorion layer, spongy layer, or some combination. Consequently, the inclusion or exclusion of layers, including the amnion, chorion, or intermediate layers of these tissues, may affect the growth factor content,<sup>9,13</sup> an important measure of the preservation of the essential composition of the native tissue. Additionally, we characterised release of growth factors and cytokines from dACM in vitro and found that 94.2% of measured factors were released over 7 days. Extended release of these factors in vitro may be beneficial; as research by Ashraf et al. has shown that in an animal model, sustained release of factors has been shown to be beneficial in supporting wound healing.<sup>20</sup>

Cell proliferation and migration is an important part of the natural wound-healing process.<sup>18</sup> Here, we have demonstrated that CM from dACM significantly increased proliferation of fibroblasts and keratinocytes and migration of fibroblasts. Growth factors identified in placental-derived tissues have been shown to be chemotactic including EGF, PDGF-BB, and TGF- $\beta$ 1 for keratinocytes,<sup>21</sup> and bFGF, TGF- $\beta$ 1, and PDGF for fibroblasts.<sup>22</sup> It is unlikely that any single growth factor or cytokine drives any of the observed in vitro effects and responses of cell types studied; rather, we hypothesize that results seen are likely because of a synergistic effect between multiple growth factors and cytokines.

Another important aspect of wound repair is cell-cell paracrine signalling within the wound microenvironment.<sup>21,23</sup> When fibroblasts and keratinocytes were exposed to dACM CM, several changes were observed in both the gene expression and protein production profiles. These included increased KGF and IL-6 production in fibroblasts and HB-EGF and IL-1Ra in keratinocytes. Both KGF and IL-6 have been shown to be upregulated in fibroblasts during co-cultures with keratinocytes<sup>23</sup>; both of these growth factors have been shown to stimulate epidermal keratinocyte cell proliferation.<sup>23</sup> HB-EGF, which has been identified in the fluid of burn wounds,<sup>24</sup> has been shown to be mitogenic for both fibroblasts and keratinocytes.<sup>21</sup> IL-1Ra is most well known as an anti-inflammatory cytokine that inhibits interleukin 1-alpha (IL-1 $\alpha$ ) and IL-1 $\beta$ , but IL-1Ra has also been shown to upregulate keratinocyte proliferation.<sup>25</sup> To our knowledge, this is the first study to systematically evaluate

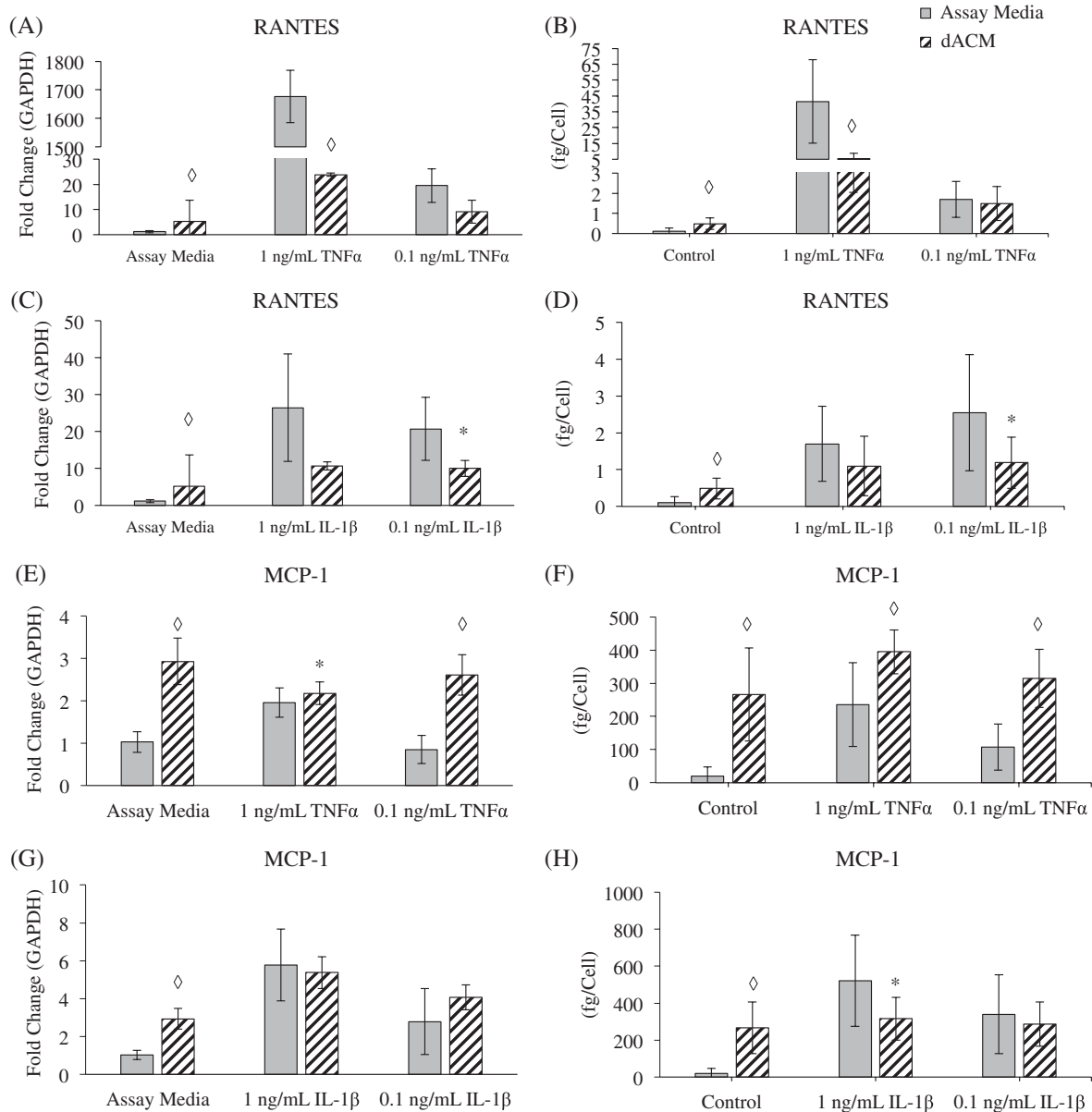


**FIGURE 6** Impact of dACM on fibroblasts stimulated with TNF- $\alpha$  and IL-1 $\beta$  cytokines. Gene expression of RANTES in fibroblasts stimulated with (A) TNF- $\alpha$  and (C) IL-1 $\beta$  normalised to GAPDH. Protein production of RANTES after stimulation with (B) TNF- $\alpha$  and (D) IL-1 $\beta$ . Gene expression of MCP-1 in fibroblasts stimulated with (E) TNF- $\alpha$  and (G) IL-1 $\beta$  normalised to GAPDH. Protein production of MCP-1 after stimulation with (F) TNF- $\alpha$  and (H) IL-1 $\beta$ . Mean  $\pm$  SD reported;  $n = 9$  for gene expression assays and  $n = 12$  for ELISAs; significance compared with respective assay media group is denoted by: \* denotes  $P < 0.05$ , \*\* denotes  $P < 0.01$ , and  $\diamond$  denotes  $P < 0.001$ . Abbreviations: dACM, dehydrated amnion/chorion membranes; GAPDH, glyceraldehyde 3-phosphate dehydrogenase; MCP-1, monocyte chemoattractant protein 1; RANTES, regulated on activation, normal T cell expressed and secreted

changes to both gene expression and protein production in response to placental-derived tissues.

Study of fibroblasts and keratinocyte downstream signalling cascades suggest that cells may respond to dACM CM through various pathways in vitro. Exposure to dACM resulted in an increase in phosphorylation of multiple intracellular pathways for fibroblasts, but keratinocyte response to dACM CM was more muted compared with fibroblasts. While this was not observed in our study, activation of the AKT and ERK  $\frac{1}{2}$  pathway was previously reported with keratinocytes when exposed to human amnion,<sup>26,27</sup> highlighting the effect composition may have on cellular signalling.

Another interesting observation was that dACM CM increased SMAD2 phosphorylation in fibroblasts and keratinocytes. SMAD2 is activated in response to the TGF- $\beta$  superfamily; these results suggest that TGF- $\beta$  may play a role in the effect of dACM CM on various cell types. However, the role is likely complicated, as a previous study has shown that exposure to amniotic membranes resulted in modified keratinocyte responses to TGF- $\beta$  stimulation in vitro.<sup>26</sup> We hypothesize that TGF- $\beta$  released from dACM may influence both keratinocytes and fibroblasts; and future studies will evaluate this interaction further. To our knowledge, this is the first study to investigate the effects of an

amnion/chorion graft and intracellular signalling of both keratinocytes and fibroblasts.

Exposure to dACM CM resulted in an altered response of fibroblasts to pro-inflammatory cytokines, although these changes are not strictly anti-inflammatory or pro-inflammatory. In the context of inflammation, addition of dACM CM was found to decrease the expression and production of pro-inflammatory cytokine RANTES, which supports prior research indicating that placental grafts downregulate inflammation.<sup>28</sup> In this work, we saw an overall upregulation of MCP-1 in response to dACM. MCP-1 is known to play a role in cell extravasation for monocytes, memory T cells, and Natural Killer cells, and MCP-1 is known to be upregulated in response to growth factors and cytokines such as VEGF, PDGF, TNF- $\alpha$ , and IFN- $\gamma$ .<sup>29</sup> Consequently, MCP-1 and the observed increase could be considered to be a pro-inflammatory response; however, MCP-1 has also been shown to have multiple anti-inflammatory effects including shifting macrophages towards the M2 (anti-inflammatory) phenotype.<sup>30</sup> In fact, placental-derived cells and tissues have been shown to stimulate M2 (or anti-inflammatory) polarisation of macrophages<sup>31</sup> and elicit anti-inflammatory responses from macrophages.<sup>28,32</sup> We hypothesize that the relationship between these tissues and inflammation modulation is complex, with the net effect likely dependent on interplay between multiple cell types. One of the biggest limitations of this study is the evaluation of cell types individually in a two-dimensional model. Future in vitro work will focus on developing and evaluating multi-cell systems in three-dimensional environments.

#### ACKNOWLEDGEMENTS

The authors would like to acknowledge the support of the University of Alabama at Birmingham's Pathology Core Research lab, in particular Dr Dezhi Wang, for their assistance with histology and immunohistochemistry. This study was supported and funded by Organogenesis, Canton MA.

#### CONFLICT OF INTEREST

J.P.M., K.A.K., M.R.K., and K.M. are employees of Organogenesis.

#### ORCID

John P. McQuilling  <https://orcid.org/0000-0003-0418-1083>

MaryRose Kammer  <https://orcid.org/0000-0002-0487-5184>

Kelly A. Kimmerling  <https://orcid.org/0000-0002-3159-5700>

Katie C. Mowry  <https://orcid.org/0000-0002-0047-544X>

#### REFERENCES

- Guariguata L, Whiting DR, Hambleton I, Beagley J, Linnenkamp U, Shaw JE. Global estimates of diabetes prevalence for 2013 and projections for 2035. *Diabetes Res Clin Pract.* 2014;103(2):137-149.
- Fortington LV, Geertzen JHB, van Netten JJ, Postema K, Rommers GM, Dijkstra PU. Short and long term mortality rates after a lower limb amputation. *Eur J Vasc Endovasc Surg.* 2013;46(1):124-131.
- Gruss JS, Jirsch DW. Human amniotic membrane: a versatile wound dressing. *Can Med Assoc J.* 1978;118(10):1237-1246.
- Branski LK, Herndon DN, Celis MM, Norbury WB, Masters OE, Jeschke MG. Amnion in the treatment of pediatric partial-thickness facial burns. *Burns.* 2008;34(3):393-399.
- Lavery L, Fulmer J, Shebetka KA, et al. The efficacy and safety of Grafix<sup>®</sup> for the treatment of chronic diabetic foot ulcers: results of a multi-centre, controlled, randomised, blinded, clinical trial. *Int Wound J.* 2014;11(5):554-560.
- DiDomenico LA, Orgill DP, Galiano RD, et al. Aseptically processed placental membrane improves healing of diabetic foot ulcerations: prospective, randomized clinical trial. *Plast Reconstr Surg Glob Open.* 2016;4(10):e1095.
- Zelen CM, Serena TE, Gould L, et al. Treatment of chronic diabetic lower extremity ulcers with advanced therapies: a prospective, randomised, controlled, multi-centre comparative study examining clinical efficacy and cost. *Int Wound J.* 2016;13(2):272-282.
- Bianchi C, Cazzell S, Vayser D, et al. A multicentre randomised controlled trial evaluating the efficacy of dehydrated human amnion/chorion membrane (EpiFix<sup>®</sup>) allograft for the treatment of venous leg ulcers. *Int Wound J.* 2018;15(1):114-122.
- Koob TJ, Lim JJ, Zabek N, Masee M. Cytokines in single layer amnion allografts compared to multilayer amnion/chorion allografts for wound healing. *J Biomed Mater Res B Appl Biomater.* 2015;103(5):1133-1140.
- Cooke M, Tan EK, Mandrycky C, He H, O'Connell J, Tseng SCG. Comparison of cryopreserved amniotic membrane and umbilical cord tissue with dehydrated amniotic membrane/chorion tissue. *J Wound Care.* 2014;23(10):465-476.
- McQuilling JP, Vines JB, Mowry KC. In vitro assessment of a novel, hypothermally stored amniotic membrane for use in a chronic wound environment. *Int Wound J.* 2017;7:1-13.
- Johnson A, Gyurdieva A, Dhall S, Danilkovitch A, Duan-Arnold Y. Understanding the impact of preservation methods on the integrity and functionality of placental allografts. *Ann Plast Surg.* 2017;79(2):203-213.
- McQuilling JP, Vines JB, Kimmerling KA, Mowry KC. Proteomic comparison of amnion and chorion and evaluation of the effects of processing on placental membranes. *Wounds.* 2017;29(6):E38-E42.
- Paolin A, Trojan D, Leonardi A, et al. Cytokine expression and ultrastructural alterations in fresh-frozen, freeze-dried and  $\gamma$ -irradiated human amniotic membranes. *Cell Tissue Bank.* 2016;17(3):399-406.
- Mowry KC, Bonvallet PP, Bellis SL. Enhanced skin regeneration using a novel amniotic-derived tissue graft. *Wounds.* 2017;29(9):277-285.
- Koob TJ, Rennert R, Zabek N, et al. Biological properties of dehydrated human amnion/chorion composite graft: implications for chronic wound healing. *Int Wound J.* 2013;10(5):493-500.
- Duan-Arnold Y, Gyurdieva A, Johnson A, Jacobstein DA, Danilkovitch A. Soluble factors released by endogenous viable cells enhance the antioxidant and chemoattractive activities of cryopreserved amniotic membrane. *Adv Wound Care.* 2015;4(6):329-338.
- Eming SA, Martin P, Tomic-Canic M. Wound repair and regeneration: mechanisms, signaling, and translation. *Sci Transl Med.* 2014;6(265):265sr6.
- Saji F, Nonaka M, Pawankar R. Expression of RANTES by IL-1 beta and TNF-alpha stimulated nasal polyp fibroblasts. *Auris Nasus Larynx.* 2000;27(3):247-252.
- Ashraf A, Lee PHU, Kim K, et al. Effect of sustained-release PDGF and TGF-beta on cyclophosphamide-induced impaired wound healing. *Plast Reconstr Surg.* 2009;124(4):1118-1124.
- Seeger MA, Paller AS. The roles of growth factors in keratinocyte migration. *Adv Wound Care.* 2015;4(4):213-224.
- Barrientos S, Stojadinovic O, Golinko MS, Brem H, Tomic-Canic M. Growth factors and cytokines in wound healing. *Wound Repair Regen.* 2008;16(5):585-601.

23. Werner S, Krieg T, Smola H. Keratinocyte-fibroblast interactions in wound healing. *J Invest Dermatol.* 2007;127(5):998-1008.
24. McCarthy DW, Downing MT, Brigstock DR, et al. Production of heparin-binding epidermal growth factor-like growth factor (HB-EGF) at sites of thermal injury in pediatric patients. *J Invest Dermatol.* 1996;106(1):49-56.
25. Kondo M, Yamato M, Takagi R, Namiki H, Okano T. The regulation of epithelial cell proliferation and growth by IL-1 receptor antagonist. *Biomaterials.* 2013;34(1):121-129.
26. Alcaraz A, Mrowiec A, Insausti CL, et al. Amniotic membrane modifies the genetic program induced by TGF $\beta$ , stimulating keratinocyte proliferation and migration in chronic wounds. *PLoS One.* 2015;10(8):e0135324.
27. Insausti CL, Alcaraz A, García-Vizcaíno EM, et al. Amniotic membrane induces epithelialization in massive posttraumatic wounds. *Wound Repair Regen.* 2010;18(4):368-377.
28. Magatti M, De Munari S, Vertua E, et al. Amniotic mesenchymal tissue cells inhibit dendritic cell differentiation of peripheral blood and amnion resident monocytes. *Cell Transplant.* 2009;18(8):899-914.
29. Eming SA, Krieg T, Davidson JM. Inflammation in wound repair: molecular and cellular mechanisms. *J Invest Dermatol.* 2007;127(3):514-525.
30. Sierra-Filardi E, Nieto C, Domínguez-Soto A, et al. CCL2 shapes macrophage polarization by GM-CSF and M-CSF: identification of CCL2/CCR2-dependent gene expression profile. *J Immunol.* 2014;192(8):3858-3867.
31. Tan JL, Chan ST, Wallace EM, Lim R. Human amnion epithelial cells mediate lung repair by directly modulating macrophage recruitment and polarization. *Cell Transplant.* 2014;23(3):319-328.
32. Guo X, Kaplunovsky A, Zaka R, et al. Modulation of cell attachment, proliferation, and angiogenesis by decellularized, dehydrated human amniotic membrane in in vitro models. *Wounds.* 2017;29(1):28-38.

#### SUPPORTING INFORMATION

Additional supporting information may be found online in the Supporting Information section at the end of this article.

**How to cite this article:** McQuilling JP, Kammer M, Kimmerling KA, Mowry KC. Characterisation of dehydrated amnion chorion membranes and evaluation of fibroblast and keratinocyte responses in vitro. *Int Wound J.* 2019;16:827–840. <https://doi.org/10.1111/iwj.13103>